UNCLASSIFIED

AD NUMBER
AD249141
NEW LIMITATION CHANGE
TO Approved for public release, distribution unlimited
FROM Distribution authorized to U.S. Gov't. agencies and their contractors; Administrative/Operational Use; OCT 1960. Other requests shall be referred to US Navy Office of Naval Research, Washington, DC 20350.
AUTHORITY
ONR ltr 9 Nov 1977

THIS PAGE IS UNCLASSIFIED

Columbia University
in the City of New York

DEPARTMENT OF CIVIL ENGINEERING
AND ENGINEERING MECHANICS
Institute of Flight Structures

444 900

11-1-5
XEROX

DIFFRACTION OF A PLANE SHOCKWAVE BY AN ARBITRARY RIGID CYLINDRICAL OBSTACLE

by

M. B. FRIEDMAN

and

R. SHAW

Office of Naval Research
Project NR 064-428
Contract Nonr 266(08)
Technical Report No. 25
CU-2-60-ONR 266(08)-CE

October 1960

Columbia University
in the City of New York

DEPARTMENT OF CIVIL ENGINEERING
AND ENGINEERING MECHANICS

Institute of Flight Structures

DIFFRACTION OF A PLANE SHOCKWAVE BY AN ARBITRARY RIGID CYLINDRICAL OBSTACLE

by

M. B. FRIEDMAN

and

R. SHAW

Office of Naval Research
Project NR 064-428
Contract Nonr 266(08)
Technical Report No. 25
CU-2-60-ONR 266(08)-CE

October 1960

SUMMARY

The two dimensional problem of the interaction of a plane weak shock wave with a cylindrical obstacle of arbitrary cross section is considered. An integral equation for the surface values of the potential is formulated and solved approximately for the case of a square box with completely rigid boundaries.

INTRODUCTION

This report is concerned with the two dimensional problem of the determination of the pressure and velocity fields resulting from the interaction of a plane weak shock wave with a cylindrical obstacle of arbitrary cross section. Such problems have been previously considered and analytical solutions for a number of simple special geometries have been found by various techniques.

The method of images has been employed to construct a solution for an infinite plane obstacle (1). Separation of variables has been used for such simple geometries as the circular cylinder (2). The problem of an infinite wedge has been solved by conformal mapping with the use of geometrical acoustics to determine the proper region of solution (3). This latter problem has also been solved for the more general case of curved wave fronts by the use of the appropriate Green's functions (4). Configurations involving sharp corners are characterised by the fact that these corners act as centers of diffraction leading to different solutions in different regions of space-time. This feature allows the construction of the solution for a box from that for an infinite wedge but the procedure is impractical for more than two corners.

Apart from such simple geometries the general problem does not appear amenable to analytical solution. The use of numerical methods based on finite differences to solve the differential equations is impractical, even with large scale computers, because of the three dimensional (two space, one time) character of the problem and the presence of discontinuities in the field.

A significant simplification can be made, however, if the problem is reformulated in terms of values of the pressure on the surface of the obstacle alone. The spatial dimensions of the problem are reduced from two to one and this remaining space dimension, if the obstacle is finite, is limited in extent. This formulation is particularly suitable for physical problems which require only a solution on the surface of the obstacle. If the solution in the field is also desired it can be constructed in a straight forward manner from the surface values.

The procedure developed here formulates an integral equation for the the pressure at an arbitrary field point in terms of the initial wave and an integral of time retarded values of the pressure and its derivatives over the surface of the obstacle. An integral equation on surface values alone is obtained by allowing the field point to approach the surface of the obstacle; values throughout the field may be obtained by direct integration over the surface values.

The effect of the discontinuity in the pressure and the velocity at the wave front on the surface can be separated from the remaining surface effects and integrated directly. The remaining integrations are approximated by assuming the surface pressure to have an average value over specified steps in space and time. The integrations are then replaced by summations which, because of the time-retarded effect lead to successive algebraic non-simultaneous equations on the unknown surface values. The fact that these equations are not simultaneous is vital because it permits the use of a large number of mesh points without prohibitive computations.

The pressure distribution on the surface of a rigid square box under a symmetric plane pulse loading is found by desk computations for time steps up to one transit time. The portions of the solution corresponding to the infinite wedge give excellent agreement with the known analytical solutions (3).

1. Initial - Boundary - Value Problem Formulation.

The pressure field that results from the interaction of a plane acoustic shock with a two-dimensional obstacle of arbitrary shape, rigid* and fixed in an acoustic medium is to be determined. For the purpose of analysis it is more convenient to consider a finite cylindrical obstacle of arbitrary length and of constant cross section rather than a two dimensional obstacle. The field corresponding to this three dimensional problem is identical in every plane section normal to the axis of the cylinder, i.e. independent of distance along the axis of the cylinder, for times less than the propagation time from the ends of the cylinder to the nearest section considered. Over these time intervals the three dimensional field provides the desired two dimensional solution. This is a consequence of the hyperbolic character of the wave equation which governs the field.

In this three dimensional field, let a cartesian coordinate system x', y', z' be introduced with the z' axis taken parallel to the generators of the cylinder. The cross section $z' = $ constant is bounded by an arbitrary piece-wise smooth curve $x'(s)$, $y'(s)$ where the parameter s is arc length along the boundary of the cross section [fig. 1]. At $t = 0$ the obstacle is subjected to a plane acoustic shock; the line of contact between the shock and the obstacle is taken as the z' axis. The incident shock represents a step in pressure whose magnitude is used to normalize the pressures which are given as differences from the pressure in the undisturbed state ahead of the shock. Consequently, the states ahead and behind the shock at $t = 0$, correspond respectively to $p = 0$ and $p = 1$ thus defining the initial state.

*The method developed in this report is applicable to the more general case of a non-rigid obstacle; see forthcoming reports.

The interaction field may be described in terms of a continuous velocity potential $\varphi\,(x,y,z,t)$ which satisfies the wave equation and is related to the pressure through $p = +\rho_o \partial\varphi/\partial t$. In terms of φ the incident shock is defined by

$$\rho_o\,\varphi(\text{WAVE}) \equiv \rho_o\,\varphi_w = \begin{cases} t - x\cos\beta - y\sin\beta & ; \; t \geqslant x\cos\beta + y\sin\beta \\ 0 & ; \; t \leqslant x\cos\beta + y\sin\beta \end{cases}$$

where $x = x'/c \;,\; y = y'/c \;,\; z = z'/c$

c being the speed of sound and β is the angle between the x axis and the normal to the incident shock front. This together with the rigid surface condition $\frac{\partial\varphi}{\partial n} = 0$, n is the normal to the obstacle surface, establishes the following initial-boundary value problem for φ.

$$\left.\begin{array}{ll}
\text{D.E.} & \Box^2\varphi = \varphi_{xx} + \varphi_{yy} + \varphi_{zz} - \varphi_{tt} = 0 \\
\text{I.C.} & \rho_o\,\varphi(x,y,z,0) = \begin{cases} t - x\cos\beta - y\sin\beta \; ; & 0 \geqslant x\cos\beta + y\sin\beta \\ 0 \; ; & 0 \leqslant x\cos\beta + y\sin\beta \end{cases} \\
 & \rho_o\,\dfrac{\partial\varphi(x,y,z,0)}{\partial t} = \begin{cases} 1 \; ; & 0 \geqslant x\cos\beta + y\sin\beta \\ 0 \; ; & 0 \leqslant x\cos\beta + y\sin\beta \end{cases} \\
\text{B.C.} & \dfrac{\partial\varphi}{\partial n}(x,y,z,t) = 0 \;;\quad x = x(s),\; y = y(s)
\end{array}\right\} (1.1)$$

Although equations (1.1) specify the problem completely, the form is not suitable for analysis when dealing with arbitrary shapes. Instead an equivalent formulation in terms of an integral equation can be developed which is more amenable to further treatment.

2. Integral Equation Formulation.

The integral equation can be developed by treating the problem as a characteristic-boundary-value problem in 4-dimensional space-time (x,y,z,t) to which Green's identity may be applied, rather than as an initial-boundary-value problem. Consider the surface formed by the intersection of the characteristic hyper-plane representing the incident front and the cylindrical hyper-surface representing the obstacle, in space-time. The union of the influence domains of all the points of the surface of intersection is a domain in 4-space exterior to which the "secondary" (disturbance) potential defined by $\varphi_s = \varphi - \varphi_w$ must vanish. The boundary of this region consists of reflection and diffraction characteristics. For φ to be a continuous solution for all (x,y,z,t), φ_s must also vanish on this boundary.

In addition to the characteristic surface, say $\Psi(x_o,y_o,z_o,t_o)$, corresponding to the secondary potential, there exists at any point (x, y,z,t), a characteristic half-cone Γ :

$$t-t_o = \left[(x-x_o)^2+(y-y_o)^2+(z-z_o)^2\right]^{1/2} = R$$

These characteristic surface, together with the obstacle surface form a closed region V in 4-space whose projection in physical space is exterior to the obstacle.

For the wave operator $\Box^2 \equiv \frac{\partial^2}{\partial x^2} + \frac{\partial^2}{\partial y^2} + \frac{\partial^2}{\partial z^2} - \frac{\partial^2}{\partial t^2}$

Green's identity takes the form

$$\iiiint_V (u\,\Box^2 v - v\,\Box^2 u)\,dx_0\,dy_0\,dz_0\,dt_0 = \iiint_S \left(v\frac{\partial u}{\partial \nu} - u\frac{\partial v}{\partial \nu}\right) dS$$

where $\frac{\partial}{\partial \nu}$ represents conormal differentiation. If now v is identified with φ_s, u taken as the progressive wave solution $u = 1 - \frac{t-t_0}{R}$, and V, S correspond to the above mentioned region and bounding surface, the identity reduces to

$$\iiint_{S'} \left(\varphi_s \frac{\partial u}{\partial \nu} - u\frac{\partial \varphi_s}{\partial \nu}\right) dS' + \iiint_{C_\epsilon} \left(\varphi_s \frac{\partial u}{\partial \nu} - u\frac{\partial \varphi_s}{\partial \nu}\right) dC = 0 \qquad (2.1)$$

C_ϵ corresponds to a hyper-cylinder of radius ϵ cut out of the region V to account for the singularity in u at r = 0; S' denotes the surface of the obstacle plus the surface of the secondary disturbance in 4-space. For the chosen function u, the integrals over C_ϵ can be reduced to

$$4\pi \int_0^t \varphi_s(x,y,z,t_0)\,(t-t_0)\,dt_0$$

In addition, on that portion of S' corresponding to the secondary front, $\varphi_s = 0$ and consequently $\frac{\partial \varphi_s}{\partial \nu} = 0$ since the front is characteristic. On the obstacle surface $\frac{\partial \varphi_s}{\partial \nu} = -\frac{\partial \varphi_s}{\partial n}$. Hence, eq. (2.1) simplifies to

$$\int_0^t \varphi_s(x,y,z,t_0)\,(t-t_0)\,dt_0 = \frac{+1}{4\pi} \iiint_{S'} \left(\varphi_s \frac{\partial u}{\partial n_0} - u\frac{\partial \varphi_s}{\partial n_0}\right) dS'$$

Differentiating both sides twice with respect to t, yields

$$\varphi_s(x,y,z,t) = \frac{1}{4\pi}\frac{\partial^2}{\partial t^2} \iint_{S_0'(x,y,z,t)} dS_0' \int_0^{t-R} \left(u\frac{\partial \varphi_s}{\partial n_0} - \varphi_s \frac{\partial u}{\partial n_0}\right) dt_0$$

Here the 4-space surface integration has been separated into a surface integration S_o over the physical surface of the obstacle with limits determined by the intersection of the cone Γ and the secondary front on the surface of the obstacle in 4-space and a time integration whose upper limit is the cone Γ.

The time differentiation may be carried through the S_o integration since the integrand vanishes along the curves of the intersection; u vanishes along Γ, while φ_s vanishes along the secondary front. Hence [1]

$$\varphi_s(x,y,z,t) = \frac{1}{4\pi} \iint\limits_{S_o(x,y,z,t)} \left[\frac{1}{R}\frac{\partial \varphi_s}{\partial n_o} + \frac{1}{R^2}\varphi_s \frac{\partial R}{\partial n_o} + \frac{1}{R}\frac{\partial \varphi_s}{\partial t_o}\frac{\partial R}{\partial n_o} \right]_{t_o = t-R} dS_o' \quad (2.2)$$

Since the solution function φ_s is uniquely determined by the specification of $\partial\varphi_s/\partial n_o$ alone, as given by eq. (1.1), it follows that eq. (2.2) represents an integral equation for φ_s.[1]

A significant simplifications can be achieved by establishing that

$$\iint\limits_{S_o} \left[\frac{1}{R}\frac{\partial \varphi_w}{\partial n_o} + \frac{1}{R^2}\varphi_w \frac{\partial R}{\partial n_o} + \frac{1}{R}\frac{\partial \varphi_w}{\partial t_o}\frac{\partial R}{\partial n_o} \right]_{t_o = t-R} dS_o' = 0 \quad (2.3)$$

for then eq. (2.2) can be written in terms of the total potential φ:[2,3]

$$\varphi(x,y,z,t) = \varphi_w + \frac{1}{4\pi} \iint\limits_{S_o'} \left[\frac{1}{R}\frac{\partial \varphi}{\partial n_o} + \frac{1}{R^2}\varphi \frac{\partial R}{\partial n_o} + \frac{1}{R}\frac{\partial \varphi}{\partial t_o}\frac{\partial R}{\partial n_o} \right]_{t_o = t-R} dS_o' \quad (2.4)$$

1. This can be considered a generalization of the classical Kirchoff's formula, the latter dealing with a physical space of fixed extent, i.e. S_o independent of time.
2. An attempt to derive this eq. for φ directly, would involve consideration of integrals over the characteristic secondary front.
3. An alternate heuristic derivation of this equation by means of Dirac delta functions is given in Appendix I.

Eq. (2.3) may be verified by extending the definition of φ or φ_s into a space time region whose projection in physical space is interior to the obstacle, by means of a saltus problem. Consider the region $\bar{V}$ in 4-space bounded by the three characteristic surfaces corresponding to the secondary front, the cone Γ and the incident wave front. This region contains an interior boundary, namely the surface of the obstacle. For $\bar{V}$ considered as a single region it is possible to define a solution φ which is discontinuous but whose normal derivative is continuous across the obstacle surface.

This solution is identical to φ in V as defined by eq. (2.2) while it vanishes in the region $\bar{V}$-V. That the latter is the correct extension follows from the condition $\varphi = 0$ on the incident front and $\frac{\partial \varphi}{\partial n} = 0$ on the obstacle-surface. This in turn implies $\varphi_s = - \varphi_w$ in $\bar{V}$-V. Consequently Green's identity may be applied to this region with $v = \varphi_s$ and $u = 1 - \frac{t-t_0}{R}$. Since the field point x,y,z,t is exterior to $\bar{V}$-V, eq. (2.3) follows.

Returning to eq. (2.4), let it be differentiated with respect to t and multiplied by ρ_0 with $\partial \varphi / \partial n_0$ set equal to zero:

$$\rho(x,y,z,t) = 1 + \frac{1}{4\pi} \frac{\partial}{\partial t} \int_{s_\ell}^{s_u} ds_0 \int_{z_{0\ell}-z}^{z_{0u}-z} dz_0 \left\{ \left[\frac{1}{R^2}(\rho_0 \varphi) + \frac{1}{R} p \right] \frac{\partial R}{\partial n_0} \right\}_{t_0 = t-R} \quad (2.5)$$

where

$$z_{0u}-z,\ z_{0\ell}-z = \pm \left[\{ t - (x_0(s) \cos\beta + y_0(s) \sin\beta) \}^2 - \{ x - x_0(s) \}^2 - \{ y - y_0(s) \} \right.$$

and $s_{0u}, s_{0\ell}$ are the roots of $(z_{0u}-z)^2 = (z_{0\ell}-z)^2 = 0$

The differentiation may be carried out to yield

$$p(x,y,t) = 1 + \frac{1}{2\pi}\int_{s_{o\ell}}^{s_{ou}} ds_o \int_0^{z_{ou}-z} \left[\frac{1}{R^2}p + \frac{1}{R}\frac{\partial p}{\partial t_o}\right]_{t_o=t-R} \frac{\partial R}{\partial n_o}\, dz_o \qquad (2.6)$$

$$+ \frac{1}{2\pi}\int_{s_{o\ell}}^{s_{ou}} ds_o \left\{\left[\frac{\partial z_{ou}}{\partial t}\right]\left[\frac{1}{R^2}(p_o\varphi) + \frac{1}{R}p\right]_{t_o=t-R}\right\}_{z_o=z_{ou}-z}$$

Here $R^2 = (x-x_o(s))^2 + (y-y_o(s))^2 + z_o^2$, so that p is independent of z. Unlike the situation encountered in obtaining eq. (2.3), the integrands of eq. (2.5) do not vanish at $z_o = z_{ou} - z$. This gives rise to the last term in eq. (2.6) which involves values of φ and p immediately behind the wave front $(z_o = z_o u - z)$ and may be interpreted as the effect on a field point of the discontinuity in the incident pressure field; it can be evaluated readily for a given $x(s)$, $y(s)$ since $\varphi(z_{ou}-z) = 0$ and $p(z_{ou}-z)$ is known.

Eq. (2.6) can be interpreted as an integral equation for the pressure. Consider its behavior as the field point (x,y) approaches the surface of the obstacle. The integrands become infinite at the point $R = 0$. By considering the behavior of the integrals in the vicinity of this point, it is readily established (appendix) that these improper integrals converge in the ordinary sense. In fact, the contribution to the double integral from the immediate vicinity of this point approaches the limit value $1/2\ p(x(s), y(s), t)$. The remaining portion from the double integral is finite and in the special case of the surface point located directly behind the wave front, this contribution vanishes. In this case the single integral also vanishes. This is in accord with the well-known results that for the interaction between a plane wave and an arbitrary obstacle, the pressure immediately behind the reflected wave front on the surface of the obstacle, is just twice the pressure behind the incident wave.

Eq. (2.6) may then be written

$$p(s,t) = 2 + \frac{1}{\pi} \lim_{\substack{S_{0\epsilon} \to [R=0] \\ S_{0\epsilon} \ni R=0}} \left\{ \iint_{S_0 - S_{0\epsilon}} dS_0 \left(\left[\frac{1}{R^2} p + \frac{1}{R} \frac{\partial p}{\partial t_0} \right]_{t_0 = t-R} \frac{\partial R}{\partial n_0} \right) + \int ds_0 \left[\frac{\partial z_{ou}}{\partial t} \right] \left[\frac{p}{R} \frac{\partial R}{\partial n_0} \right]_{\substack{t_0 = t-R \\ z_0 = z_{ou} - z}} \right\} \quad (2.7)$$

The procedure employed in solving eq. (2.7) for $p(s,t)$ involves the approximation of the double integration as follows. Let $p(s,t)$ be assumed to have a constant mean value over fixed intervals in s and t. Associated with these intervals are specific regions in s_o and z_o in which p is constant. In addition let $\frac{\partial p}{\partial t_o}$ be replaced by a backward difference in time. Then the double integral can be approximated by a double summation of time retarded values of p, whose coefficients are integrals of $\frac{1}{R} \frac{\partial R}{\partial n_o}$ and $\frac{1}{R^2} \frac{\partial R}{\partial n_o}$ over the associated regions in s_o and z_o. These latter integrals can be evaluated for a given obstacle shape. With this approximation, eq. (2.7) can be applied to successive intervals in s, t to yield a set of successive algebraic equations for the mean values of p. The details of this method are illustrated in section 3 where a box-shaped obstacle is considered.

Computations have indicated that, since the major contribution to p is made by the terms in eq. (2.7) which can be evaluated exactly, the values of $p(s,t)$ obtained in this manner are relatively insensitive to the magnitude of the fixed intervals (provided $\frac{\Delta t}{\Delta s} < 1$). It is anticipated that this will be the case in general.

3. Solution for the Case of a Box-Shaped Obstacle

The specific configuration for which eq. (2.7) has been solved is a square box whose boundaries are defined by S_1: $x = 0$, S_2: $y = 0$, S_3: $y = a$, S_4: $x = a$. The direction of motion of the incident wave is chosen for convenience of symmetry, to be such that the normal to the front coincides with a diagonal of the square, i.e. $\beta = \pi/4$ (fig. 2). In this case eq. (2.7) takes the form

$$p^i(s,t) = 2 + 2\sum_{\substack{j=1\\ \neq i}}^{4} {}_iB^j + \frac{1}{\pi}\sum_{\substack{j=1\\ \neq i}}^{4} \int_{s_{ol}}^{s_{ou}} ds_o \int_0^{z_{ou}-z} dz_o \left[\frac{p^j}{R_j^2} + \frac{1}{R_j}\frac{\partial p^j}{\partial t_o}\right]_{t_o = t-R_j} \left(\frac{\partial R_j}{\partial n_o}\right)$$

with $\quad {}_iB^j = \frac{(p^j)_{z_{ou}-z}}{2\pi} \int_{s_{ol}}^{s_{ou}} ds_o \left[\frac{\partial z_{ou}}{\partial t}\frac{1}{R_j}\frac{\partial R_j}{\partial n_{oj}}\right]_{z_{ou}-z = z_o}$

The symbol i refers to the surface S_i containing the point s, at which the pressure is p^i. S_i is not included in the integrations since the expressions containing $\lim\limits_{R\to 0}$ vanish for a surface of constant curvature (appendix II). In the expression for ${}_iB^j$, the term p^j is equal to the constant two for $j = 1, 2$ and is equal to zero for $j = 3, 4$ (see appendix II). The regions of integration in s_o, z_o on each surface are determined by the ellipses:

$$S_{1,2}: \quad t - s_o/\sqrt{2} = R(s_o, z_o, x, y)$$
$$S_{3,4}: \quad t - a/\sqrt{2} - s_o/\sqrt{2} = R(s_o, z_o, x, y)$$

with the restructions that for $s_{ou} > a$, s_{ou} is set equal to a and for $s_{ol} < 0$, s_{ol} is set equal to zero.

The double integral is approximated by assuming $p^j(s,t)$ to have the constant value $p_k^j(t-\ell+1)$ over the space-time interval $(k-1)/\sqrt{2} < s_o < k/\sqrt{2}$, $t-\ell < t_o < t-\ell+1$). The time derivative $\frac{\partial p}{\partial t_o}$ is approximated by a backwards difference in time, $p_k^j(t-\ell+1) - p_k^j(t-\ell)$. For points s_o swept over by the incident front within the time interval being considered, the derivative is replaced by $p_k^j(t_o)-2$ for $j = 1, 2$ or $p_k^j(t_o)-0$ for $j = 3,4$. The integration may then be replaced by a double summation over k and ℓ in which the coefficients of $p_k^j(t_o)$ are known integrals.

It is also convenient to modify slightly the regions of integration in s_o, z_o in order to reduce the number of coefficients of p_k^j that need to be computed. For this purpose, the regions of integration are approximated by:

$$t = R(z_o, s_o, x, y) \text{ on } \quad S_i \qquad i = 1, 2, 3, 4$$

with the previous restrictions on s_{ou}, s_{ol} still valid and p^j_k being defined as zero in the region exterior to the ellipses $t - s_o/\sqrt{2} = R$, $t - s/\sqrt{2} = R$, i.e. ahead of the wave front. The coefficients obtained in this manner are in fact the same for any orientation of the incident front relative to the box.

It then follows that the approximate system to be solved is given by:

$$p^i_m(t) \equiv p^i\left(\tfrac{2m-1}{2}\sqrt{2}, t\right) = \lambda + \lambda \sum_{\substack{j=1\\ \neq i}}^{2} {}_iB^j + \sum_{\substack{j=1\\ \neq i}}^{4} \sum_{l=1}^{t} \sum_{k=1}^{P} \Big\{ p^j_k(t-l+1)\, {}_iq^j_{kl}(m) + \left[p^j_k(t-l+1)\right]' {}_ir^j_{kl}(m) \Big\} \qquad (2.7)$$

$${}_iq^j_{kl}(m) = \frac{1}{\pi} \int_{(k-1)\sqrt{2}}^{k\sqrt{2}} ds_{oj} \int_{\sqrt{(l-1)^2-(x-x_o)^2-(y-y_o)^2}}^{\sqrt{l^2-(x-x_o)^2-(y-y_o)^2}} dz_o \left\{ \frac{1}{R_j^2} \frac{\partial R_j}{\partial n_{oj}} \right\}_{s = \frac{2m-1}{2}\sqrt{2}}$$

$${}_ir^j_{kl}(m) = \frac{1}{\pi} \int_{(k-1)\sqrt{2}}^{k\sqrt{2}} ds_{oj} \int_{\sqrt{(l-1)^2-(x-x_o)^2-(y-y_o)^2}}^{\sqrt{l^2-(x-x_o)^2-(y-y_o)^2}} dz_o \left\{ \frac{1}{R_j} \frac{\partial R_j}{\partial n_{oj}} \right\}_{s = \frac{2m-1}{2}\sqrt{2}}$$

$\left[p^j_k(t-l+1)\right]' =$ $p^j_k(t-l+1) - p^j_k(t-l)$ if wave has not passed over point k between $t-l$ and $t-l+1$; otherwise

$p^j_k(t-l+1) - \lambda$ on $j = 1, 2$

$p^j_k(t-l+1) - 0$ on $j = 3, 4$

where P is the number of space intervals per side.

At each time step t and space point* m on S_i eq. (2.7) relates $p_m^i(t)$ to values of $\dot{p}$ corresponding to earlier times. Hence as previously indicated the system of equations obtained are successive rather than simultaneous. Only at the corners do two adjacent space points have an opportunity to interact within a single time interval. Consequently, at each corner, at each time step there occur two simultaneous equations. The numerical results obtained for the choice of eight space steps on each side of the box and sixteen time steps corresponding to one transit time are listed in tables I and II and figs. (3,4).

4. Discussion of Results.

In the case of the box, the solution in certain regions of space-time may be identified with known solutions obtained by geometric acoustics [3]. For example, for $t < a/\sqrt{2}$ the solution along $S_{1,2}$ coincides with the solution for an infinite wedge of vertex angle $\pi/2$ formed by $S_{1,2}$. Consequently the results for $S_{1,2}$ for the first eight time steps may be compared with the analytic solution given in [3]. Since in this case the solution depends only upon $\frac{x}{t}$, $\frac{y}{t}$, a comparison of values at all time steps may be made simultaneously and the convergence of the values for increasing time may be examined. The results for the eighth time step are plotted along with the exact solution in fig. (3) and the agreement is excellent; the greatest error is less than 3%.

A further estimate of the accuracy of the numerical solution may be gained by a comparison with the rigid box solution given in ref. [5]. Again the agreement is excellent.

*The field point is taken in the center of the space interval at $\frac{2m-1}{2}\sqrt{2}$

Examination of fig.(4) indicate that the steady state solution of $\rho = 1$ everywhere appears to be approached rapidly even within the interval of one transit time.

REFERENCES

(1) P.M. Morse and H. Feshbach-Methods of Theoretical Physics Vol. 1 p. 848 McGraw Hill Book Company 1953.

(2) R.D. Mindlin and H.H. Bleich-Response of an Elastic Cylindrical Shell to a Transverse Step Shock Wave; Journal of Applied Mechanics Vol. 20 No. 2 June 1953, p. 189.

(3) J. Keller and A. Blank-Diffraction and Reflection of Pulses by Wedges and Corners; Comm. on Pure and Applied Math. June 1951.

(4) M.B. Friedman-The Method of the Green's Function Applied to the Diffraction of Pulses; Tech. Rept. No. 18, CU-18-56 ONR-266(08) C.E.

(5) M.B. Friedman-Acoustic Pulse Loading on a Two Dimensional Rigid Box in the Vicinity of a Free Surface; Tech. Rept. No. 22, CU-1-59 ONR-266(08) C.E.

(6) B.B. Baker and E.T. Copson- The Mathematical Theory of Huygens' Principle, Oxford Press 1939.

TABLE OF VALUES ON FRONT FACE OF RIGID BOX

UNDER SYMMETRIC PULSE: $p(t) = \frac{\partial \varphi}{\partial t}$

t								
1	1.40							
2	1.38	2.00						
3	1.34	1.55	2.00					
4	1.32	1.38	1.67	2.00				
5	1.36	1.35	1.50	1.88	2.00			
6	1.34	1.42	1.38	1.64	2.00	2.00		
7	1.33	1.36	1.45	1.44	1.73	2.00	2.00	
8	1.34	1.38	1.39	1.48	1.53	1.83	2.00	2.00
9	1.34	1.35	1.41	1.44	1.51	1.65	2.00	1.87
10	1.34	1.36	1.40	1.43	1.47	1.51	1.75	1.62
11	1.34	1.35	1.38	1.39	1.47	1.52	1.36	1.33
12	1.34	1.36	1.37	1.40	1.42	1.39	1.24	1.12
13	1.34	1.35	1.37	1.37	1.41	1.24	1.15	1.06
14	1.34	1.35	1.37	1.39	1.25	1.18	1.04	1.09
15	1.34	1.35	1.36	1.26	1.22	1.05	1.10	1.07
16	1.34	1.35	1.31	1.21	1.07	1.09	1.05	1.03
	1	2	3	4	5	6	7	8

First Diffraction at Upper Corner

Second Diffraction at Upper Corner

TABLE OF VALUES ON REAR SURFACE OF RIGID BOX

UNDER SYMMETRIC PULSE

9	0.49							
10	0.93							
11	1.17	0.63						
12	1.20	0.89	0.53					
13	1.07	0.94	0.62	0.07				
14	1.04	1.03	0.83	0.46				
15	1.00	0.98	0.92	0.70	0.36			
16	0.99	0.93	0.86	0.79	0.59	0.24		
	9	10	11	12	13	14	15	16

Second Diffraction at Upper Corner

First Diffraction at Upper Corner

Appendix I

Introduce the fundamental solution to the three dimensional wave equation

$$g(\bar{r},t;\bar{r}_0,t_0) = \frac{\delta[(t-t_0)-R]}{R}$$

which satisfies

$$\nabla^2 g - \frac{\partial^2 g}{\partial t^2} = -4\pi\,\delta(t-t_0)\,\delta(\bar{r}-\bar{r}_0)$$

where $R = |\bar{r}-\bar{r}_0|$, $\bar{r} = (x,y,z)$ a field point, $\bar{r}_0 = (x_0,y_0,z_0)$ a source point and δ is the Dirac delta function in one, three or four dimensions as required.

The secondary "disturbance" potential $\varphi_s = \varphi - \varphi_w$ also satisfies the wave equation

$$\nabla^2 \varphi_s - \frac{\partial^2 \varphi_s}{\partial t^2} = 0$$

with initial conditions: $\varphi_s = \dfrac{\partial \varphi_s}{\partial t} = 0$ at $t = 0$

Consequently the following equation is true

$$\iiiint_{V_0^{(4)}} dV_0^{(4)} \left\{ g\,\nabla_0^2 \varphi_s - \varphi_s \nabla_0^2 g - g\frac{\partial^2 \varphi_s}{\partial t_0^2} + \varphi_s \frac{\partial^2 g}{\partial t_0^2} \right\} = \begin{cases} 4\pi\varphi_s \\ 0 \end{cases}$$

where $V_0^{(4)}$ is a four dimensional volume in space time and the right hand side is $4\pi\varphi_s$ if the point $\bar{r} = \bar{r}_0$, $t = t_0$ is included in $V_0^{(4)}$ and 0 if it is not.

Two different regions of integration are employed. They are both bounded by the initial time plane $t_0 = 0$, the incident wave plane $t_0 + x_0\cos\beta - y_0\sin\beta = 0$ the obstacle surface extended into space time and a surface which will include the characteristic cone $(t-t_0)-R = 0$ in the volume of integration. Due to the singular behavior of the integrand, all contributions come from the surface $(t-t_0)-R = 0$ within the region of integration. One region of integration is taken exterior to and the other interior to the obstacle surface.

Consider first, for either region $V_0^{(4)}$, the term

$$\iiiint dV_0^{(4)} \left\{ \varphi_s \frac{\partial^2 g}{\partial t_0^2} - g \frac{\partial^2 \varphi_s}{\partial t_0^2} \right\} = \iiint dV_0^{(3)} \int_{t_0=0}^{t_0=t+\epsilon} dt_0 \left\{ \varphi_s \frac{\partial^2 g}{\partial t_0^2} - g \frac{\partial^2 \varphi_s}{\partial t_0^2} \right\}$$

$$= \iiint dV_0^{(3)} \left[\varphi_s \frac{\partial g}{\partial t_0} - g \frac{\partial \varphi_s}{\partial t_0} \right]_{t_0=0}^{t_0=t+\epsilon} = 0$$

since g and $\frac{\partial g}{\partial t_0}$ vanish for every value of $t < t_0$ and φ_s and $\frac{\partial \varphi_s}{\partial t_0}$ are both 0 at $t_0 = 0$.

The remainder of the integral is

$$\iiiint dV_0^{(4)} \left\{ g \nabla_0^2 \varphi_s - \varphi_s \nabla_0^2 g \right\}$$

$$= \int_{t_0=0}^{t_0=t+\epsilon} dt_0 \iiint dV_0^{(3)} \left\{ g \nabla_0^2 \varphi_s - \varphi_s \nabla_0^2 g \right\}$$

$$= \int_{t_0=0}^{t_0=t+\epsilon} dt_0 \iint_{S_0} dS_0 \left[g \frac{\partial \varphi_s}{\partial n_0} - \varphi_s \frac{\partial g}{\partial n_0} \right]$$

by Green's Theorem where S_0 is the surface bounding the physical space volume of integration $V_0^{(3)}$ and n_0 is the outward normal to S_0.

Adding the two integrals corresponding to these two regions of integration will give an equation on $\varphi_s(\bar{r}, t)$ in terms of a discontinuity in φ_s across the obstacle surface since the normal, n_0, is opposite in sign in the two integrations.

$$4\pi \varphi_s = \int_{t_0=0}^{t_0=t+\epsilon} dt_0 \iint_{S_0} dS_0 \left\{ g \frac{\partial [\varphi_s]}{\partial n_0} - [\varphi_s] \frac{\partial g}{\partial n_0} \right\}$$

where [ ] represents the discontinuity value and $+n_0$ is taken toward the interior of the obstacle in physical space.

Since φ_w is continuous, the discontinuity in φ_s must be identical to the discontinuity in φ. As seen in the text, the interior value of φ is zero and the discontinuity in φ is therefore just the value immediately exterior to the obstacle surface.

$$4\pi (\varphi - \varphi_w) = \int_{t_0=0}^{t_0=t+\epsilon} dt_0 \iint_{S_0} dS_0 \left\{ g \frac{\partial \varphi}{\partial n_0} - \varphi \frac{\partial g}{\partial n_0} \right\}$$

Because of the behavior of g, the time integration can be taken thru the surface integration and carried out giving Eq. (2.4).

$$\varphi = \varphi_w + \frac{1}{4\pi}\iint_{S_0} dS_0 \left[\frac{1}{R}\frac{\partial \varphi}{\partial n_0} + \left(\frac{1}{R^2}\varphi + \frac{1}{R}\frac{\partial \varphi}{\partial t_0}\right)\frac{\partial R}{\partial n_0}\right]_{t_0 = t-}$$

Appendix II-a

The immediate neighborhood of a point on any curved surface may be considered plane as an approximation which becomes exact as the neighborhood shrinks to the point. To find the pressure field at a point immediately behind the wave front on an obstacle surface, it is therefore sufficient to consider the interaction of the wave front with an infinite plane obstacle. The result obtained will of course be equally useful in the specific example of the square box for the two planes which compose the "front" of the box. The integral equation is still valid but now is applied only to S_1

$$\varphi(\bar{r},t) = \varphi_w(\bar{r},t) + \frac{1}{4\pi}\iint_{S_0} dz_0\, dy_0 \left\{ \frac{\varphi^1}{R^2} + \frac{F^1}{R}\right\}\left(\frac{\partial R}{\partial n_0}\right)_{t_0 = t-R}$$

As $\bar{r}$ approaches a point on S_1, x approaches zero. However, $\left.\frac{\partial R}{\partial n_0} = -\frac{x}{R}\right]_{x}$ must also approach zero except at the indeterminate point R = 0, i.e. the location of the field point on the surface. To avoid this indeterminary the point R = 0 is removed from the integration by distorting the surface in the neighborhood of R = 0 from a plane to a semisphere of radius ρ about R = 0. Over this surface $\frac{\partial R}{\partial n_0} = 1$. The integration is then in two parts; the semisphere and the remainder of the plane surface. The latter integration is zero since $\frac{\partial R}{\partial n_0}$ is zero and the former integration is

$$\lim_{\rho = R \to 0} \iint_{\substack{\text{Semi-} \\ \text{Sphere}}} \left[\frac{\varphi^1}{R^2} + \frac{p^1}{R} \right]_{t_0 = t - R} (1) R^2 d\Omega = 2\pi \varphi^1(\bar{r}, t)$$

Since in the limit, the terms $\varphi^1(\bar{r}_0, t_0)$ and $p^1(\bar{r}_0, t_0)$ can be removed from the integration and evaluated at $t_0 = t$, $R = 0$.

$$\therefore \quad \varphi^1(\bar{r}, t) = \frac{1}{\rho_0}\left[t - x\cos\beta - y\sin\beta\right]_{x=0} + \frac{1}{2}\varphi^1(\bar{r}, t)$$

$$\varphi^1(\bar{r}, t) = 2(t - y\sin\beta)/\rho_0$$

$$p^1(\bar{r}, t) = 2$$

Appendix II-b

Behind the wave front on each of the rear surfaces of the square box exists a region in space time which is not influenced by any of the corners of the box. The integrations required to determine the pressure in these regions from Eq. (2.7) are then taken only over the neighboring front surface with values for p on that surface corresponding to the infinite plane solution. For example, consider a point on surface $i = 3$

$$p^3(\bar{r}, t) = 2 + 2\,{}_3B^1 + \frac{2}{\pi} \iint_{S_1 (x_0 = 0)} dz_0\, dy_0 \left\{ \frac{1}{R^2} \frac{\partial R}{\partial x_0} \right\}$$

with integration limits given by

$$t - y_0/\sqrt{2} = \left. \sqrt{(a - y_0)^2 + (x - x_0)^2 + z_0^2} \right]_{x_0 = 0}$$

The term $2\,{}_iB^j$ is left in integral form for convenience.

$$2\,{}_3B^1 = -\frac{2x}{\pi} \int_{y_{0L}}^{y_{0u}} dy_0 \left[\frac{1}{(t - y_0/\sqrt{2}) \sqrt{(t - y_0/\sqrt{2})^2 - (a - y_0)^2 - x^2}} \right]$$

where the limits of integration are the roots of

$$(t - y_0/\sqrt{2})^2 - (a - y_0)^2 - x^2 = 0$$

This follows from the fact that $y_{o\ell}$ must be greater than zero while y_{ou} must be less than a in order that the ends of the front surface (i.e. corners) will not play any role in the integration.

The double integral is reduced to a single integral.

$$\lim_{x_0 \to 0} \frac{2}{\pi} \int_{y_{o\ell}}^{y_{ou}} dy_0 \int_0^{z_{ou} = \sqrt{(t-y_0/\sqrt{2})^2 - (a-y_0)^2 - x^2}} dz_0 \left\{ \frac{1}{[z_0^2 + (x-x_0)^2 + (a-y_0)^2]} \frac{(x - x_0)}{\sqrt{z_0^2 + (x-x_0)^2 + (a-y_0)^2}} \right\}$$

$$= -\frac{2x}{\pi} \int_{y_{o\ell}}^{y_{ou}} dy_0 \left\{ \frac{\sqrt{(t-y_0/\sqrt{2})^2 - (a-y_0)^2 - x^2}}{(x^2 + (a-y_0)^2)\ (t - y_0/\sqrt{2})} \right\}$$

Combining this integral with the term $2_3 B'$ gives

$$-\frac{2x}{\pi} \int_{y_{o\ell}}^{y_{ou}} dy_0 \left\{ \frac{(t - y_0/\sqrt{2})}{(x^2 + (a-y_0)^2) \sqrt{(t - y_0/\sqrt{2})^2 - (a-y_0)^2 - x^2}} \right\}$$

$$= \quad -2$$

$$\therefore \quad p^3 = 2 - 2 = 0$$

The region in which this solution will be valid on the rear surface S_3 is $t < x < t/\sqrt{2}$ from $t < x$ corresponding to $a - y_0 > 0$ and $x < t/\sqrt{2}$ limiting points to those behind the wave front.

Appendix III

The expressions for the ${}_iB^j$ obtained by integration are given below together with the conditions under which each expression is valid. These conditions are obtained from the limits in the integral expressions for the ${}_iB^j$ and may be interpreted in terms of geometric acoustic theory as representing the diffraction effects produced by the corners of the box.

$$ {}_iB^j = \frac{1}{\pi}\int_{s_{0\ell}}^{s_{0u}} ds_0 \left[\frac{\partial z_{0u}}{\partial t}\right]\left[\frac{1}{R_j}\frac{\partial R_j}{\partial m_0}\right]_{z_0 = z_{0u} - z} \quad ; \quad j = 1,2 $$

$$ {}_1B^2 = 0 \; ; \qquad \boxed{t^2 \leq y_m^2} $$

$$ {}_1B^2 = \frac{-y_m}{\pi\sqrt{t^2+\frac{1}{2}y_m^2}}\left\{\frac{\pi}{2} - \sin^{-1}\left[\frac{y_m^2}{\sqrt{2}\,t\sqrt{t^2-\frac{1}{2}y_m^2}}\right]\right\} ; \qquad \boxed{\left(t-\frac{a}{\sqrt{2}}\right)^2 \leq a^2 + y_m^2} $$

$$ {}_1B^2 = -\frac{y_m}{\pi\sqrt{t^2+\frac{1}{2}y_m^2}}\left\{\sin^{-1}\left[\frac{at + y_m^2/\sqrt{2}}{(t-a/\sqrt{2})\sqrt{t^2-\frac{1}{2}y_m^2}}\right] - \sin^{-1}\left[\frac{y_m^2}{\sqrt{2}\,t\sqrt{t^2-\frac{1}{2}y_m^2}}\right]\right\} ; $$

$$ \boxed{\left(t-\frac{a}{\sqrt{2}}\right)^2 > a^2 + y_m^2} $$

$$ {}_3B^1 = 0 \; ; \qquad \boxed{\left(t-\frac{a}{\sqrt{2}}\right)^2 < \frac{1}{2}x_m^2} $$

$$ {}_3B^1 = {}_3B^1_u - {}_3B^1_L \; ; \qquad \boxed{\left(t-\frac{a}{\sqrt{2}}\right)^2 \geq \frac{1}{2}x_m^2} $$

$$ {}_3B^1_u = \frac{-x_m}{\pi\sqrt{(t-\frac{a}{\sqrt{2}})^2+\frac{1}{2}x_m^2}}\left\{\frac{\pi}{2}\right\} ; \qquad \boxed{(t-a/\sqrt{2})^2 \leq x_m^2} $$

$$ {}_3B^1_u = -\frac{x_m}{\pi\sqrt{(t-\frac{a}{\sqrt{2}})^2+\frac{1}{2}x_m^2}}\left\{\sin^{-1}\frac{x_m^2/\sqrt{2}}{(t-a/\sqrt{2})\sqrt{(t-\frac{a}{\sqrt{2}})^2-\frac{1}{2}x_m^2}}\right\} ; \qquad \boxed{(t-a/\sqrt{2})^2 \geq x_m^2} $$

$$ {}_3B^1_L = \frac{-x_m}{\pi\sqrt{(t-\frac{a}{\sqrt{2}})^2+\frac{1}{2}x_m^2}}\left\{-\frac{\pi}{2}\right\} ; \qquad \boxed{t^2 < x_m^2 + a^2} $$

$$ {}_3B^1_L = \frac{-x_m}{\pi\sqrt{(t-\frac{a}{\sqrt{2}})^2+\frac{1}{2}x_m^2}}\left\{\sin^{-1}\left[\frac{(t-a/\sqrt{2})^2+\frac{1}{2}x_m^2 - t(t-a/\sqrt{2})}{(t/\sqrt{2})\sqrt{(t-a/\sqrt{2})^2-\frac{1}{2}x_m^2}}\right]\right\} ; \qquad \boxed{t^2 > x_m^2 + a^2} $$

$$ {}_3B^1 = 0\,; \qquad \boxed{\left(t-\tfrac{x_m}{\sqrt{2}}\right)^2 < \tfrac{1}{2}a^2} $$

$$ {}_3B^2 = {}_3B^2_u - {}_3B^2_L\,; \qquad \boxed{\left(t-\tfrac{x_m}{\sqrt{2}}\right)^2 \geq \tfrac{1}{2}a^2} $$

$$ {}_3B^2_u = \frac{-a}{\pi\sqrt{\left(t-\frac{x_m}{\sqrt{2}}\right)^2+\frac{1}{2}a^2}}\left\{\frac{\pi}{2}\right\}; \qquad \boxed{\left(t-\tfrac{a}{\sqrt{2}}\right)^2 < (a-x_m)^2+a^2} $$

$$ {}_3B^2_u = \frac{-a}{\pi\sqrt{\left(t-\frac{x_m}{\sqrt{2}}\right)^2+\frac{1}{2}a^2}}\left\{\sin^{-1}\left[\frac{\left(t-\frac{x_m}{\sqrt{2}}\right)^2+\frac{1}{2}a^2-\left(t-\frac{x_m}{\sqrt{2}}\right)\left(t-\frac{a}{\sqrt{2}}\right)}{\frac{1}{\sqrt{2}}\left(t-\frac{a}{\sqrt{2}}\right)\sqrt{\left(t-\frac{x_m}{\sqrt{2}}\right)^2-\frac{1}{2}a^2}}\right]\right\}; \qquad \boxed{\left(t-\tfrac{a}{\sqrt{2}}\right)^2 \geq (a-x_m)^2+a^2} $$

$$ {}_3B^2_L = \frac{-a}{\pi\sqrt{\left(t-\frac{x_m}{\sqrt{2}}\right)^2+\frac{1}{2}a^2}}\left\{-\frac{\pi}{2}\right\}; \qquad \boxed{t^2 \leq x_m^2+a^2} $$

$$ {}_3B^2_L = \frac{-a}{\pi\sqrt{\left(t-\frac{x_m}{\sqrt{2}}\right)^2+\frac{1}{2}a^2}}\left\{\sin^{-1}\left[\frac{\left(t-\frac{x_m}{\sqrt{2}}\right)^2+\frac{1}{2}a^2-t\left(t-\frac{x_m}{\sqrt{2}}\right)}{\frac{1}{\sqrt{2}}\,t\sqrt{\left(t-\frac{x_m}{\sqrt{2}}\right)^2-\frac{1}{2}a^2}}\right]\right\}; \qquad \boxed{t^2 \geq x_m^2+a^2} $$

The coefficients ${}_iq^j_{kl}(m)$ and ${}_ir^j_{kl}(m)$ must satisfy the following symmetry conditions.

$$
\begin{aligned}
{}_1q^2_{kl}(Y_m) &= {}_1q^2_{kl}(Y_m) \\
{}_1q^3_{kl}(Y_m) &= {}_1q^2_{kl}(a-Y_m) \\
{}_1q^4_{kl}(Y_m) &= {}_1q^4_{kl}(Y_m)
\end{aligned}
\qquad
\begin{aligned}
{}_3q^1_{kl}(X_m) &= {}_1q^2_{(p+1-k)l}(Y_m) \\
{}_3q^2_{kl}(X_m) &= {}_1q^4_{kl}(Y_m) \\
{}_3q^4_{kl}(X_m) &= {}_1q^2_{(p+1-k)l}(a-Y_m)
\end{aligned}
$$

$$
\begin{aligned}
{}_2q^1_{kl}(X_m) &= {}_1q^2_{kl}(Y_m) \\
{}_2q^3_{kl}(X_m) &= {}_1q^4_{kl}(Y_m) \\
{}_2q^4_{kl}(X_m) &= {}_1q^2_{kl}(a-Y_m)
\end{aligned}
\qquad
\begin{aligned}
{}_4q^1_{kl}(Y_m) &= {}_1q^4_{kl}(Y_m) \\
{}_4q^2_{kl}(Y_m) &= {}_1q^2_{(p+1-k)l}(Y_m) \\
{}_4q^3_{kl}(Y_m) &= {}_1q^2_{(p+1-k)l}(a-Y_m)
\end{aligned}
$$

and a similar set for ${}_i\Omega^j_{k\ell}(m)$ where X_m or $Y_m = \frac{2m-1}{2}\sqrt{2}$ and p is the number of steps in space per side.

Therefore only four sets of coefficients need be computed for each value of m. The integral expressions for the coefficients are simplified by using a constant average value in place of R_j over each region of integration. As R_j can never be zero on any of the surfaces of integration and is practically constant over all separate regions of integration except those near the corners this approximation is quite good. Values near the corners must be obtained without this approximation.

$$ {}_1q^2_{k\ell}(m) \simeq \frac{-Y_m}{\pi \bar{R}^3} \left\{ \left[{}_1Q^2_{k\ell} - {}_1Q^2_{k(\ell-1)} \right] - \left[{}_1Q^2_{(k-1)\ell} - {}_1Q^2_{(k-1)(\ell-1)} \right] \right\} $$

$$ {}_1q^4_{k\ell}(m) \simeq \frac{-a}{\pi \bar{R}^3} \left\{ \left[{}_1Q^4_{k\ell} - {}_1Q^4_{k(\ell-1)} \right] - \left[{}_1Q^4_{(k-1)\ell} - {}_1Q^4_{(k-1)(\ell-1)} \right] \right\} $$

$$ {}_1\Omega^2_{k\ell}(m) \simeq \bar{R} \cdot {}_1q^2_{k\ell}(m) $$

$$ {}_1\Omega^4_{k\ell}(m) \simeq \bar{R} \cdot {}_1q^4_{k\ell}(m) $$

$$ \bar{R} \simeq \ell - \tfrac{1}{2} $$

$$ \begin{aligned} {}_1Q^2_{k\ell}(m) &= \tfrac{1}{2} \left[\sqrt{2}\, k \sqrt{\ell^2 - Y_m^2 - 2k^2} + (\ell^2 - Y_m^2) \sin^{-1} \frac{\sqrt{2}\,k}{\sqrt{\ell^2 - Y_m^2}} \right]; \quad \boxed{\ell^2 - Y_m^2 - 2k^2 > 0} \\ &= \tfrac{1}{2} (\ell^2 - Y_m^2) \left(\tfrac{\pi}{2}\right); \quad \boxed{\ell^2 - Y_m^2 - 2k^2 < 0,\ \ell^2 - Y_m^2 - 2(k-1)^2 > 0} \\ &= 0; \quad \boxed{\ell^2 - Y_m^2 - 2(k-1)^2 < 0} \end{aligned} $$

$$ \begin{aligned} {}_1Q^4_{k\ell}(m) &= \tfrac{1}{2} \Big[(\sqrt{2}\,k - Y_m) \sqrt{\ell^2 - a^2 - (\sqrt{2}\,k - Y_m)^2} + (\ell^2 - a^2) \sin^{-1}\left(\frac{k\sqrt{2} - Y_m}{\sqrt{\ell^2 - a^2}} \right) \\ &\quad + Y_m \sqrt{\ell^2 - a^2 - Y_m^2} + (\ell^2 - a^2) \sin^{-1} \frac{Y_m}{\sqrt{\ell^2 - a^2}} \Big]; \quad \boxed{\ell^2 - a^2 - 2k^2 > 0} \\ &= \tfrac{1}{2} (\ell^2 - a^2) \left(\tfrac{\pi}{2}\right); \quad \boxed{\ell^2 - a^2 - 2k^2 < 0,\ \ell^2 - a^2 - 2(k-1)^2 > 0} \\ &= 0; \quad \boxed{\ell^2 - a^2 - 2(k-1)^2 < 0} \end{aligned} $$

Appendix IV

It is of interest to note that the pressure at the corner of an infinite rigid wedge of arbitrary angle α may be found exactly from the integral equation

$$\varphi = \varphi_w + \frac{1}{4\pi} \iint_{S_0} dS_0 \left\{ \frac{1}{R^2} \varphi + \frac{1}{R} p \right\}_{t_0 = t-R} \left(\frac{\partial R}{\partial n_0} \right)$$

Since $\frac{\partial R}{\partial n_0}$ is zero on both surfaces for a field point at the corner $\bar{r} = a$ the only contribution comes from the point R = 0 as in appendix IIa although only a portion $\frac{\alpha}{2\pi}$ of the semi-sphere is required to exclude the corner point from the surface of integration in this case.

$$\varphi \Big]_{\bar{r}=0} = \varphi_w \Big]_{\bar{r}=0} + \frac{1}{4\pi} \left[\frac{\alpha}{2\pi} 4\pi \; \varphi \right]_{\bar{r}=0}$$

$$\varphi \Big]_{\bar{r}=0} = \frac{2\pi}{2\pi - \alpha} \; \varphi_w \Big]_{\bar{r}=0}$$

$$p \Big]_{\bar{r}=0} = \frac{2\pi}{2\pi - \alpha}$$

which is an agreement with the known infinite rigid wedge solution.

$$p \Big]_{\bar{r}=0} = \frac{4}{3} \qquad \text{for } \alpha = \pi/2$$

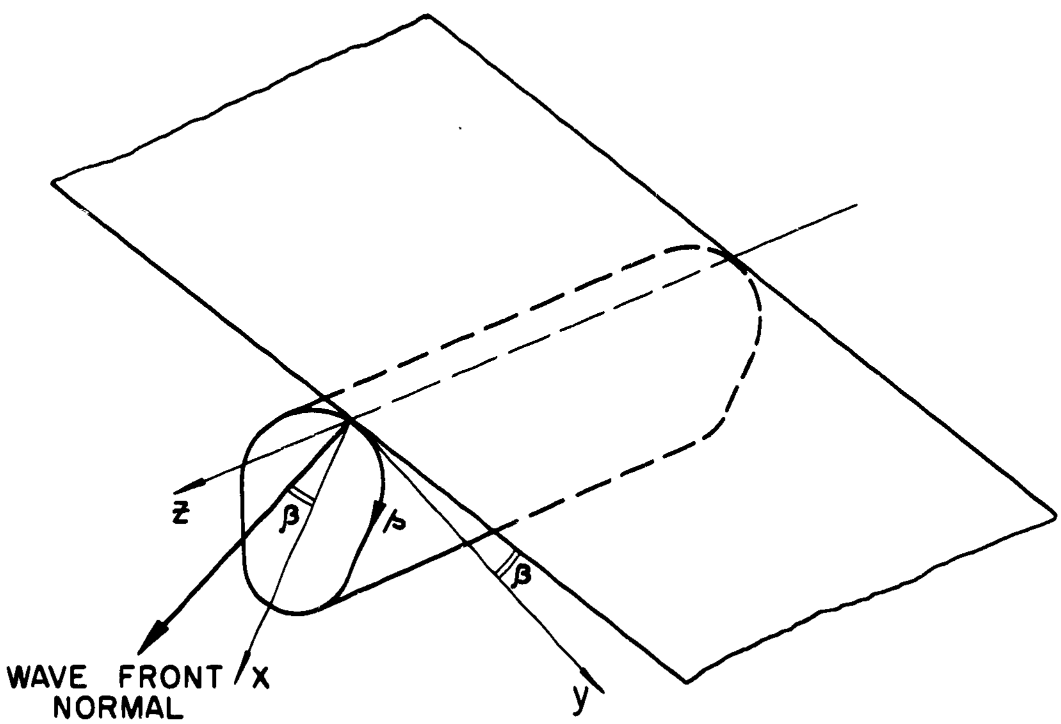

FIG.1 CONFIGURATION AT t = 0

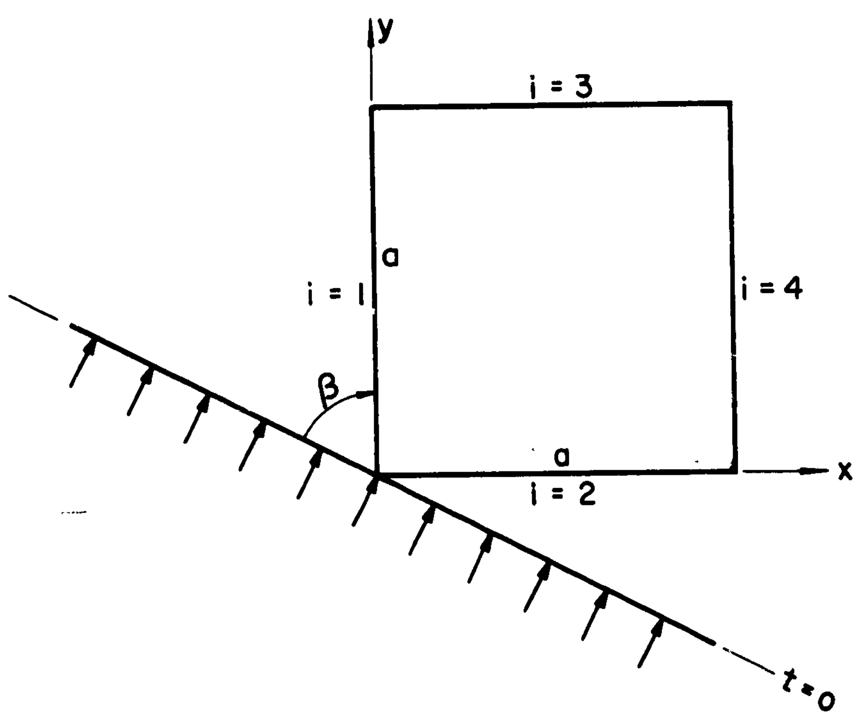

FIG.2 BOX SHAPED OBSTACLE

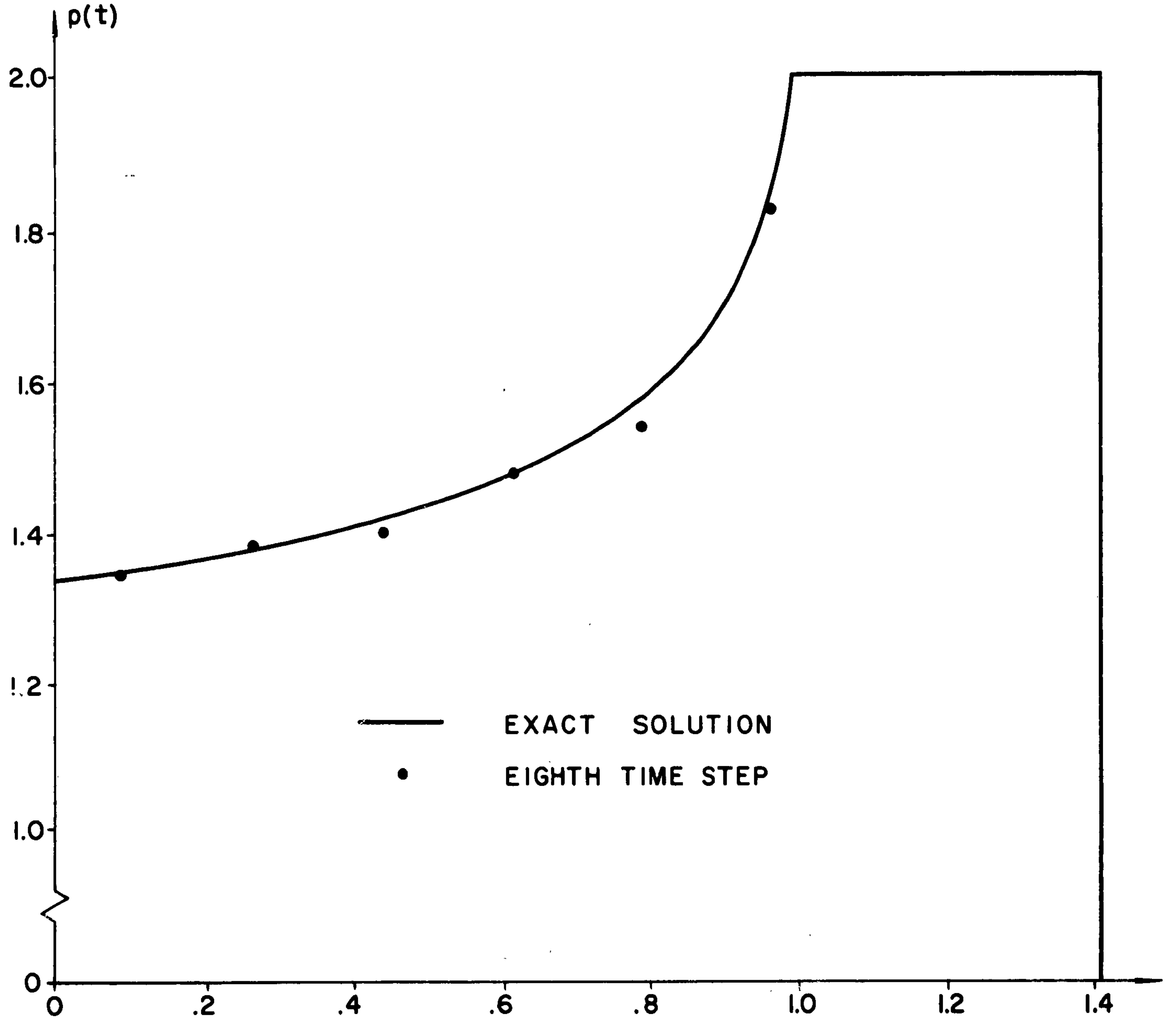

FIG. 3 SURFACE PRESSURE FOR INFINITE WEDGE

$\beta = \frac{\pi}{4}$

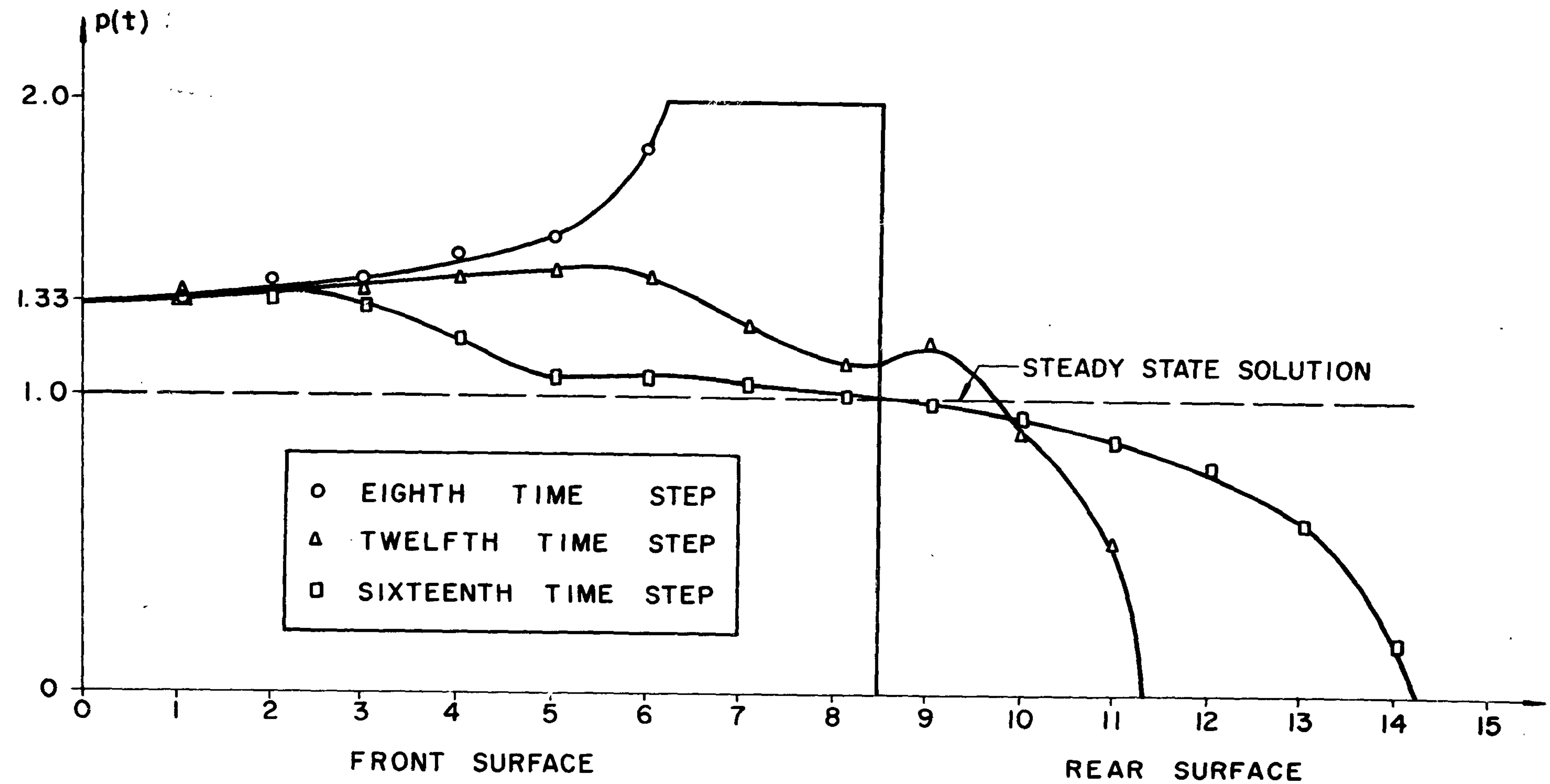

FIG. 4 SURFACE PRESSURE FOR SQUARE OBSTACLE

$\beta = \frac{\pi}{4}$

DISTRIBUTION LIST

PART A: ADMINISTRATIVE AND LIAISON ACTIVITIES

Chief of Naval Research
Department of the Navy
Washington 25, D. C.
Attn: Code 418 (1)
Code 438 (2)

Commanding Officer
Office of Naval Research
Branch Office
John Crerar Library Building
86 E. Randolph Street
Chicago 11, Illinois (1)

Commanding Officer
Office of Naval Research
Branch Office
346 Broadway
New York 13, N. Y. (1)

Commanding Officer
Office of Naval Research
Branch Office
1030 E. Green Street
Pasadena, California (1)

Commanding Officer
Office of Naval Research
Navy #100, % Fleet Post Office
New York, N. Y. (2)

Director
Naval Research Laboratory
Washington 25, D. C.
Attn: Tech. Info. Officer (6)
Code 6200 (1)
Code 6205 (1)
Code 6250 (1)
Code 6260 (1)
Code 2029 (1)

Armed Services Technical Information Agency
Arlington Hall Station
Arlington 12, Virginia (10)

Office of Technical Services
Department of Commerce
Washington 25, D. C. (1)

PART B: THE U.S. DEPARTMENT OF DEFENSE

Office of the Secretary of Defense
Research and Development Division
The Pentagon
Washington 25, D. C.
Attn: Technical Library (1)

Chief, Defense Atomic Support Agency
The Pentagon
Washington 25, D. C.
Attn: Document Library Branch (2)

Commanding General
Field Command
AFSWP, P.O. Box 5100
Albuquerque, New Mexico (3)

ARMY

Office of the Secretary of the Army
The Pentagon
Washington 25, D. C.
Attn: Army Library (1)

Chief of Staff
Department of the Army
Washington 25, D. C.
Attn: Development Branch (R&D Div.) (1)
Research Branch (R&D Div.) (1)
Special Weapons Branch (R&D Div.) (1)

Office of the Chief of Engineers
Asst. Chief for Military Construction
Department of the Army
Bldg. T-7, Gravelly Point
Washington 25, D. C.
Attn: Library Branch (1)
Structural Branch (Engr. Div.) (1)
Protective Construction Br. (Pl., Engr., & Contracts) (1)

Chief, Research and Development
Department of the Army
Washington 25, D. C.
Attn: Special Weapons & Air Defense Division (1)

Chief of Engineers
Department of the Army
Washington 25, D. C.
Attn: ENGNB (1)

Commanding General
Aberdeen Proving Ground
Maryland
Attn: Director, Ballistic Research Laboratories (2)

Commanding Officer, Engineer Research & Development Lab.
Fort Belvoir, Virginia
Attn: Chief, Tech. Intelligence Br. (1)

Director, Waterways Experiment Station
P.O. Box 631
Vicksburg, Miss.
Attn: Library (1)

Commanding Officer
Engineer Research Development Laboratory
Fort Belvoir, Virginia (1)

Office of the Chief of Ordnance
Department of the Army
Washington 25, D. C.
Attn: Research and Materials Branch (Ord. R&D Div.) (1)
ORDTX - AR (1)

Office of the Chief Signal Officer
Department of the Army
Washington 25, D. C.
Attn: Engineering & Technical Div. (1)

Commanding Officer
Watertown Arsenal
Watertown, Massachusetts
Attn: Laboratory Division (1)

Commanding Officer
Frankford Arsenal
Bridesburg Station
Philadelphia 37, Pennsylvania
Attn: Laboratory Division (1)

Office of Ordnance Research
2127 Myrtle Drive
Duke Station
Durham, North Carolina
Attn: Division of Engineering Sciences (1)

NAVY

Chief of Naval Operations
Department of the Navy
Washington 25, D. C.
Attn: Op 37 (1)
Op 36 (1)
Op 03EG (1)

Commandant, Marine Corps
Headquarters, U.S. Marine Corps
Washington 25, D. C. (1)

Chief, Bureau of Ships
Department of the Navy
Washington 25, D. C.
Attn: Code 327 (2)
Code 348 (1)
Code 371 (1)
Code 420 (2)
Code 423 (2)
Code 442 (2)
Code 421 (1)

Chief, Bureau of Aeronautics
Department of the Navy
Washington 25, D. C.
Attn: AD-2 (1)
AD-22 (1)
RS-7 (1)
TD-42 (1)

Chief, Bureau of Ordnance
Department of the Navy
Washington 25, D. C.
Attn: Ad3 (1)
Re (1)
Re3 (1)
Re5 (1)
ReN (1)

Director of Naval Intelligence
Navy Department
Washington 25, D. C.
Attn: Op-922V (1)

Chief, Bureau of Yards and Docks
Department of the Navy
Washington 25, D. C.
Attn: Code D-213 (1)
Code D-222 (1)
Code D-410C (1)
Code D-440 (1)
Code D-500 (1)

Commanding Officer and Director
David Taylor Model Basin
Washington 7, D. C.
Attn: Code 140 (1)
Code 600 (1)
Code 700 (1)
Code 720 (1)
Code 725 (1)
Code 731 (1)
Code 740 (2)

Commander
U.S. Naval Ordnance Laboratory
White Oak, Maryland
Attn: Technical Library (2)
Technical Evaluation Department (1)
EE (1)
EH (1)
R (1)

Director
Material Laboratory
New York Naval Shipyard
Brooklyn 1, New York (1)

Commanding Officer and Director
U.S. Naval Electronics Laboratory
San Diego 52, California (1)
Attn: Code 4223 (1)

Officer-in-Charge
Naval Civil Engineering Research
Naval Civil Engineering Research and Evaluation Laboratory
U.S. Naval Construction Battalion Center
Port Hueneme, California (2)
Attn: Code 753 (1)

Director
Naval Air Experimental Station
Naval Air Material Center
Naval Base
Philadelphia 12, Pennsylvania
Attn: Materials Laboratory (1)
Structures Laboratory (1)

Officer-in-Charge
Underwater Explosion Research Division
Norfolk Naval Shipyard
Portsmouth, Virginia
Attn: Dr. A. H. Keil (2)

Commander
U. S. Naval Providing Grounds
Dahlgren, Virginia (1)

Superintendent
Naval Gun Factory
Washington 25, D. C. (1)

Commander
Naval Ordnance Test Station
Inyokern, China Lake, California
Attn: Physics Division (1)
Mechanics Branch (1)

Commander
Naval Ordnance Test Station
Underwater Ordnance Division
3202 E. Foothill Boulevard
Pasadena 8, California
Attn: Structures Division (1)

Commanding Officer and Director
Naval Engineering Experiment Station
Annapolis, Maryland (1)

Superintendent
Naval Post Graduate School
Monterey, California (1)

Commandant
Marine Corps Schools
Quantico, Virginia
Attn: Director, Marine Corps Development Center (1)

AIR FORCE

Commanding General
U. S. Air Force
Washington 25, D. C.
Attn: Research and Development Division (1)

Commander
Air Material Command
Wright-Patterson Air Force Base
Dayton, Ohio
Attn: MCREX-B (1)
Structures Division (1)
WCOSI (1)

Commander
U. S. Air Forece Institute of Technology
Wright-Patterson Air Force Base
Dayton, Ohio
Attn: Chief, Applied Mechanics Group (1)

Director of Intelligence
Headquarters, U.S. Air Force
Washington 25, D. C
Attn: P.V. Branch(Air Targets Div.) (1)
AFOIN-1B2 (2)

Commander
Air Research and Development Command
P. O. Box 1395
Baltimore 3, Maryland
Attn: RDMPE (1)

Commander
Wright Air Development Center
Wright-Patterson Air Force Base
Dayton, Ohio
Attn: Dynamics Branch (1)
Aircraft Laboratory (1)
WCLSY (1)

Commanding Officer
USNNOEU
Kirtland Air Force Base
Albuquerque, New Mexico
Attn: Code 20
(Dr. J.N. Brennan) (1)

PART C: OTHER GOVERNMENT ACTIVITIES

U.S. Atomic Energy Commission
Washington 25, D. C.
Attn: Director of Research (2)

Director
National Bureau of Standards
Washington 25, D. C.
Attn: Division of Mechanics (1)
Engineering Mechanics Sec. (1)
Aircraft Structures (1)

Commandant
U.S. Cost Guard
1300 E Street, N.W.
Washington 25, D. C.
Attn: Chief, Testing and Development Division (1)

U.S. Maritime Administration
General Administration Office Bldg.
Washington 25, D. C.
Attn: Chief, Division of Preliminary Design (1)

National Advisory Committee for Aeronautics
1512 H Street, N. W.
Washington 25, D. C.
Attn: Loads and Structures Div. (2)

Director
Langley Aeronautical Laboratory
Langley Field, Virginia
Attn: Structures Division (2)

Director
Forest Products Laboratory
Madison, Wisconsin (1)

Civil Aeronautics Administration
Department of Commerce
Washington 25, D. C.
Attn: Chief, Airframe and Equipment Branch (1)

National Sciences Foundation
1520 H Street, N. W.
Washington, D. C.
Attn: Engineering Sciences Div. (1)

National Academy of Science
2101 Constitution Avenue
Washington 25, D. C.
Attn: Technical Director, Committee on Ships' Structural Design (1)
Executive Secretary, Committee on Undersea Warfare (1)

Director, Operations Research Office
Johns Hopkins University
7100 Connecticut Avenue
Chevy Chase, Maryland
Washington 15, D. C. (1)

Dr. Alvin C. Graves, Director
J-Division, Los Alamos Scientific Laboratory
P.O. Box 1663
Los Alamos, New Mexico (1)

U.S. Atomic Energy Commission
Classified Technical Library
Technical Information Service
1901 Constitution Avenue, N.W.
Washington, D. C.
Attn: Mrs. Jean M. O'Leary
For: Dr. Paul C. Fine (1)

U.S. Atomic Energy Commission
Classified Technical Library
Technical Information Service
1901 Constitution Avenue, N.W.
Washington, D. C.
Attn: Mrs. Jean M. O'Leary (1)

Sandia Corporation, Sandia Base
Albuquerque, New Mexico
Attn: Dr. Walter A. MacNair (1)

Legislative Reference Service
Library of Congress
Washington 25, D. C.
Attn: Dr. E. Wenk (1)

U.S. Atomic Energy Commission
1901 Constitution Avenue, N. W.
Washington, D.C. (1)

Massachusetts Institute of Technology
Cambridge 39, Massachusetts
Attn: Dr. Charles H. Norris (1)

PART D: INVESTIGATORS ACTIVELY ENGAGED IN RELATED RESEARCH

Professor Lynn S. Beedle
Fritz Engineering Laboratory
Lehigh University
Bethlehem, Pennsylvania (1)

Professor R. L. Bisplinghoff
Dept. of Aeronautical Engineering
Massachusetts Institute of Technology
Cambridge 39, Massachusetts (1)

Professor H. H. Bleich
Department of Civil Engineering
Columbia University
New York 27, N. Y. (1)

Professor B.A. Boley
Department of Civil Engineering
Columbia University
New York, N. Y. (1)

Professor G.F. Carrier
Pierce Hall
Harvard University
Cambridge 38, Massachusetts (1)

Professor J.E. Cermak
Dept. of Civil Engineering
Colorado State Univ.
Fort Collins, Colorado

Professor Herbert Deresiewicz
Department of Civil Engineering
Columbia University
632 W. 125th Street
New York 27, N. Y. (1)

Professor Lloyd Donnell
Department of Mechanics
Illinois Institute of Technology
Technology Center
Chicago 16, Illinois (1)

Professor D. C. Drucker, Chairman
Division of Engineering
Brown University
Providence 12, Rhode Island (1)

Professor A. C. Eringen
Department of Aeronautical Engineering
Purdue University
Lafayette, Indiana (1)

Professor W. Flugge
Department of Mechanical Engineering
Stanford University
Stanford, California (1)

Mr. Martin Goland
Midwest Research Institute
4049 Pennsylvania Avenue
Kansas City 2, Missouri (1)

Professor J. N. Goodier
Dept. of Mechanical Engineering
Stanford University
Stanford, California (1)

Professor L. E. Goodman
Engineer Experiment Station
University of Minnesota
Minneapolis, Minnesota (1)

Professor W. J. Hall
Dept. of Civil Engineering
University of Illinois
Urbana, Illinois

Professor M. Hetenyi
The Technological Institute
Northwestern University
Evanston, Illinois (1)

Professor P. G. Hodge
Department of Aeronautical Engineering
and Applied Mechanics
Polytechnic Institute of Brooklyn
99 Livingston Street
Brooklyn 2, N. Y.

Professor N. J. Hoff
Stanford University
Stanford, California (1)

Professor W. H. Hoppmann, II
Department of Mechanical Engineering
Johns Hopkins University
Baltimore, Maryland (1)

Professor Bruce G. Johnston
University of Michigan
Ann Arbor, Michigan (1)

Professor J. Kempner
Department of Aeronautical Engineering
and Applied Mechanics
Polytechnic Institute of Brooklyn
99 Livingston Street
Brooklyn 2, New York (1)

Professor H. L. Langhaar
Department of Theoretical and
Applied Mechanics
University of Illinois
Urbana, Illinois (1)

Professor B.J. Lazan, Director
Engineering Experiment Station
University of Minnesota
Minneapolis 14, Minnesota (1)

Professor E. H. Lee
Division of Applied Mathematics
Brown University
Providence 12, Rhode Island (1)

Professor George H. Lee
Director of Research
Rensselaer Polytechnic Institute
Troy, New York (1)

Mr. M. M. Lemcoe
Southwest Research Institute
8500 Culebra Road
San Antonio 6, Texas (1)

Professor Paul Lieber
Geology Department
Rensselaer Polytechnic Institute
Troy, New York (1)

Professor Hsu Lo
School of Engineering
Purdue University
Lafayette, Indiana (1)

Professor R. D. Mindlin
Department of Civil Engineering
Columbia University
632 W. 125th Street
New York 27, N. Y. (1)

Dr. A. Nadai
136 Cherry Valley Road
Pittsburgh 21, Pennsylvania (1)

Professor Paul M. Naghdi
Department of Mechanical
Engineering
University of California
Berkeley, California (1)

Professor William A. Nash
Department of Engineering
Mechanics
University of Florida
Gainesville, Florida (1)

Professor N. M. Newmark
Department of Civil Engineering
University of Illinois
Urbana, Illinois (1)

Professor Aris Phillips
Department of Civil Engineering
15 Prospect Street
Yale University
New Haven, Connecticut (1)

Professor W. Prager, Chairman
Physical Sciences Council
Brown University
Providence 12, Rhode Island (1)

Professor E. Reissner
Department of Mathematics
Massachusetts Institute of Technology
Cambridge 39, Massachusetts (1)

Professor M. A. Sadowsky
Department of Mechanics
Rensselaer Polytechnic Institute
Troy, New York

Dr. B. W. Shaffer
Dept. of Mechanical Engineering
New York University
45 Fourth Avenue
New York 53, New York (1)

Professor C. B. Smith
College of Arts and Sciences
Department of Mathematics
Walker Hall
University of Florida
Gainesville, Florida (1)

Professor J. Stallmeyer
Department of Civil Engineering
University of Illinois
Urban, Illinois (1)

Professor Eli Sternberg
Brown University
Providence, Rhode Island (1)

Professor S.P. Timoshenko
School of Engineering
Stanford University
Stanford, California (1)

Professor A.A. Velestos
Department of Civil Engineering
University of Illinois
Urbana, Illinois (1)

Professor Enrico Volterra
Department of Engineering Mech
Mechanics
University of Texas
Austin 12, Texas (1)

Professor Dana Young
Yale University
New Haven, Connecticut (1)

Project Staff (10)

For your future distribution (10)